Asymmetric Fano resonance analysis in indirectly coupled microresonators

Yun-Feng Xiao,[1,*] Min Li,[1,2] Yong-Chun Liu,[1] Yan Li,[1] Xiudong Sun,[2,†] and Qihuang Gong[1,‡]
[1] *State Key Lab for Mesoscopic Physics, Department of Physics, Peking University, Beijing 100871, People's Republic of China*
[2] *Department of Physics, Harbin Institute of Technology, Harbin 150001, People's Republic of China*
(Received 16 October 2010; published 29 December 2010; corrected 5 January 2011)

We reveal that there exists an indirect interaction between two single-mode microcavities which have no direct coupling. This indirect interaction is mediated by coupling the two microcavities to a common waveguide, and it plays a key role in obtaining the asymmetric Fano line shape of the transport spectrum of the coupled cavity system. Finally, we show that this sharp Fano line shape can contribute to highly sensitive sensing, which is immune to most environmental variations.

DOI: 10.1103/PhysRevA.82.065804 PACS number(s): 42.50.Gy, 42.60.Da, 42.79.−e

As a ubiquitous phenomenon, Fano resonance [1] was first proposed to study the autoionizing states of atoms. The shape of this resonance is distinctly asymmetric, different from conventional symmetric Lorentzian resonance curves. Since its discovery, it has been observed in different systems, including plasmonic nanoparticles, photonic crystals, plasmonic nanostructures, and electromagnetic metamaterials (for a review, see [2]). This asymmetric resonance profile essentially results from the interference between a continuum and an embedded discrete level.

Recently, optical microresonator structures with high-quality factors have attracted increasing interest for fundamental physics and device applications [3]. As many of these structures involve coupling of one or several cavities to a waveguide, such coupling systems naturally exhibit Fano resonances. The sharp Fano resonances in these systems, sometimes behaving like coupled-resonator-induced transparency, were first introduced in Refs. [4,5]. Since then, different waveguide-cavity structures have been studied theoretically and experimentally. For instance, the Lorentzian line shape can be dramatically deformed by coupling two individual microcavities [6–8], inserting two partially reflecting elements in the light path [9–11], utilizing a multimode waveguide as the external coupler to a single-mode microcavity [12], and involving at least two resonant modes in a single microcavity [13,14]. In general, coupled-resonator structures have two typical geometries: directly [6] and indirectly [7] coupled resonators. It is evident that the direct coupling structure can exhibit Fano resonances. However, in an indirect coupling structure, the interaction mechanism to produce Fano resonance has yet not been revealed, to the best of our knowledge, although the scattering matrix or transfer matrix is convenient to calculate the transport in this structure [5]. In this paper, we theoretically study a system consisting of two single-mode microcavities which have no direct coupling but are side coupled to a common waveguide (see Fig. 1). We reveal that there does exist indirect interaction between them. This indirect interaction plays the center role in obtaining the asymmetric Fano line shape of the system.

Under the rotating-wave approximation, the Hamiltonian of the system can be written as ($\hbar = 1$) [15]

$$H = \sum_{j=1,2}\left\{\omega_j c_j^\dagger c_j + \sum_{p=\pm}\int_{-\infty}^{+\infty}\omega a_{j,p}^\dagger(\omega)a_{j,p}(\omega)\,d\omega + i\sum_{p=\pm}\int_{-\infty}^{+\infty}d\omega\kappa_j(\omega)[a_{j,p}^\dagger(\omega)c_j - c_j^\dagger a_{j,p}(\omega)]\right\}, \quad (1)$$

where the first two terms represent the free Hamiltonians of the cavity and on-site waveguide modes, respectively, and the last term describes the coupling between them. Here c_j ($c_j^\dagger$) is the annihilation (creation) operator associated with the mode of the jth cavity, with resonant frequency ω_j. $a_{j,p}(\omega)$ [$a_{j,p}^\dagger(\omega)$] denotes the annihilation (creation) operator for the waveguide mode coupled to the jth cavity, with the commutation relation $[a_{j,p}(\omega), a_{j,p}^\dagger(\omega')] = \delta(\omega-\omega')$, and the subscript $p = \pm$ represents two propagating directions of waveguide modes. The coefficient $\kappa_j(\omega)$ describes the coupling between the jth cavity and the on-site waveguide modes. The Heisenberg equations of motion for the cavity and waveguide modes are

$$\frac{dc_j}{dt} = -i\omega_j c_j - \sum_{p=\pm}\int_{-\infty}^{+\infty}d\omega\kappa_j(\omega)a_{j,p}(\omega), \quad (2)$$

$$\frac{da_{j,p}(\omega)}{dt} = -i\omega a_{j,p}(\omega) + \kappa_j(\omega)c_j. \quad (3)$$

Now, by integrating Eq. (3), we can obtain the operator of the waveguide mode,

$$a_{j,p}(\omega) = e^{-i\omega(t-t_0)}A_{j,p}(\omega) + \kappa_j(\omega)\int_{t_0}^{t}e^{-i\omega(t-t')}c_j(t')\,dt', \quad (4)$$

where $A_{j,p}(\omega)$ denotes the value of $a_{j,p}(\omega)$ at $t = t_0$. With Eq. (4), substituting $a_{j,p}(\omega)$ in Eq. (2), and by taking the intrinsic decay rate $\gamma_{0,j}$ of the jth cavity mode into account (which can be obtained by following the established procedures of the Weisskopf-Wigner approximation [15]), we achieve

$$\frac{dc_j}{dt} = -i\omega_j c_j - \frac{\gamma_{0,j}}{2}c_j - \sum_{p=\pm}\int_{-\infty}^{+\infty}d\omega\kappa_j(\omega) \times\left(e^{-i\omega(t-t_0)}A_{j,p}(\omega) + \kappa_j(\omega)\int_{t_0}^{t}e^{-i\omega(t-t')}c_j(t')\,dt'\right). \quad (5)$$

*yfxiao@pku.edu.cn
†xdsun@hit.edu.cn
‡qhgong@pku.edu.cn

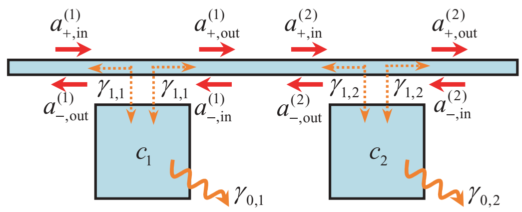

FIG. 1. (Color online) Schematic structure of two single-mode standing-wave microcavities side coupled to a common waveguide. The two cavities are separated by a long enough distance L. The parameters are defined in the text.

Since $\int_{-\infty}^{+\infty} d\omega e^{-i\omega(t-t')} = 2\pi\delta(t-t')$ and $\int_{t_0}^{t} c_j(t')\delta(t-t')\,dt = c_j(t)/2$, with the first Markov approximation $\kappa_j(\omega) = (\gamma_{1,j}/2\pi)^{1/2}$, Eq. (5) can be simplified as

$$\frac{dc_j}{dt} = -i\omega_j c_j - \frac{\gamma_{0,j}+2\gamma_{1,j}}{2}c_j - \sqrt{\gamma_{1,j}}\sum_{p=\pm} a^{(j)}_{p,\mathrm{in}}(t), \quad (6)$$

where $a^{(j)}_{p,\mathrm{in}}(t)$ describes the input field of the jth cavity mode, with the form

$$a^{(j)}_{p,\mathrm{in}}(t) = \frac{1}{\sqrt{2\pi}}\int_{-\infty}^{+\infty} A_{j,p}(\omega)e^{-i\omega(t-t_0)}d\omega. \quad (7)$$

With the input-output formula of the cavity, we have

$$a^{(j)}_{p,\mathrm{out}}(t) = a^{(j)}_{p,\mathrm{in}}(t) + \sqrt{\gamma_{1,j}}c_j, \quad (8a)$$

$$a^{(2)}_{+,\mathrm{in}}(t) = e^{i\theta}a^{(1)}_{+,\mathrm{out}}(t), \quad (8b)$$

$$a^{(2)}_{-,\mathrm{out}}(t) = e^{-i\theta}a^{(1)}_{-,\mathrm{in}}(t), \quad (8c)$$

with the propagating phase factor $\theta = k(\omega)L$, where $k(\omega)$ is the waveguide's dispersion and L denotes the waveguide distance between the coupling regions of the two microcavities. Thus, by assuming that there is no input from the right port, that is, $a^{(2)}_{-,\mathrm{in}}(t) = 0$, Eq. (6) can be rewritten as

$$\frac{dc_1}{dt} = -i\omega_1 c_1 - \frac{\gamma_{0,1}+2\gamma_{1,1}}{2}c_1 - e^{i\theta}\sqrt{\gamma_{1,1}\gamma_{1,2}}c_2 - \sqrt{\gamma_{1,1}}a^{(1)}_{+,\mathrm{in}}(t), \quad (9a)$$

$$\frac{dc_2}{dt} = -i\omega_2 c_2 - \frac{\gamma_{0,2}+2\gamma_{1,2}}{2}c_2 - e^{i\theta}\sqrt{\gamma_{1,1}\gamma_{1,2}}c_1 - \sqrt{\gamma_{1,2}}e^{i\theta}a^{(1)}_{+,\mathrm{in}}(t). \quad (9b)$$

Equations (9a) and (9b) are the most important results of this paper. It is not difficult to find that there does exist indirect interaction between the two microcavities, with the effective coupling parameter $e^{i\theta}\sqrt{\gamma_{1,1}\gamma_{1,2}}$. This interaction is similar to the strong coupling of two distant dipoles mediated by a common nanofiber [16] or a cavity mode [17].

We are interested in the transport property in the frequency domain of the indirectly coupled microcavities. To facilitate the discussion, we also suppose that each cavity has the same dissipation, that is, $\gamma_{0,j} = \gamma_0$ and $\gamma_{1,j} = \gamma_1$. From Eqs. (8a)–(8c), we achieve the whole transmission and reflection amplitudes,

$$a^{(2)}_{+,\mathrm{out}} = e^{i\theta}\left(a^{(1)}_{+,\mathrm{in}} + \sqrt{\gamma_1}c_1\right) + \sqrt{\gamma_1}c_2, \quad (10a)$$

$$a^{(1)}_{-,\mathrm{out}} = e^{i\theta}\sqrt{\gamma_1}c_2 + \sqrt{\gamma_1}c_1, \quad (10b)$$

respectively, where $c_j(\omega)$ can be obtained by neglecting all the fluctuations, setting $dc_j/dt = 0$, and taking the expectation value with respect to the steady state of Eqs. (9a) and (9b). In addition, it should be noted that the transmission and reflection are coincident with the results obtained by the transmission matrix [9].

Now we further investigate the line shape of the reflection spectrum defined by $R \equiv |r|^2 \equiv |a^{(1)}_{-,\mathrm{out}}/a^{(1)}_{+,\mathrm{in}}|^2$. Under the resonant condition ($\omega_1 = \omega_2 \equiv \omega_0$), we have the reflection coefficient

$$r = e^{i\theta}(-r_1 + r_2), \quad (11a)$$

$$r_1 = \frac{-\gamma_1(1+\cos\theta)}{i(\Delta\omega - \gamma_1\sin\theta) - \gamma_1(1+\cos\theta) - \gamma_0/2}, \quad (11b)$$

$$r_2 = \frac{-\gamma_1(1-\cos\theta)}{i(\Delta\omega + \gamma_1\sin\theta) - \gamma_1(1-\cos\theta) - \gamma_0/2}, \quad (11c)$$

where $\Delta\omega \equiv \omega - \omega_0$. In Eqs. (11), the total reflection coefficient has been intentionally written in the form of the interference of two new resonances with frequencies $\omega'_{1,2} = \omega_0 \pm \gamma_1\sin\theta$, and $\gamma_1(1\pm\cos\theta)$ describes the modified waveguide coupling strengths, respectively. These two new resonances can also be defined from Eqs. (9) as the strong indirect interaction between the original two modes should result in two new orthogonal resonant modes. It is not difficult to find that the reflection spectrum strongly depends on the propagating phase factor θ. Three cases are considered in the following.

(i) When $\theta = m\pi$ with m being an integral number, the two new resonances are degenerate ($\omega'_{1,2} = \omega_0$). In this case, either r_1 or r_2 vanishes, and the total reflection $R = |2\gamma_1/(i\Delta\omega - 2\gamma_1 - \gamma_0/2)|^2$. Thus the reflection spectrum has a symmetric Lorentz line shape but with a broadened linewidth $4\gamma_1 + \gamma_0$, as shown in Fig. 2.

(ii) When $\theta = m\pi + \pi/2$, we have $\cos\theta = 0$ and $\sin\theta = \pm1$. In this case, the total reflection can be expressed as $R = |\sum_{p=\pm}\gamma_1/[i(\Delta\omega + p\gamma_1) - \gamma_1 - \gamma_0/2]|^2$. Thus, the

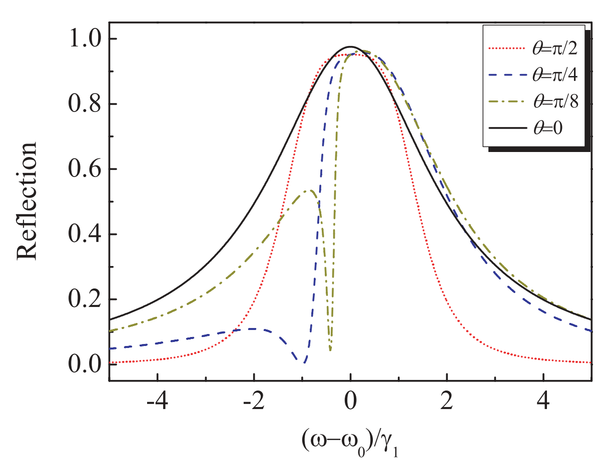

FIG. 2. (Color online) Total reflection spectra $R(\omega - \omega_0)$ of two indirectly coupled microcavities. The solid, dash-dotted, dashed, and dotted curves correspond to the cases of the propagation phase factors $\theta = m\pi$, $m\pi + \pi/8$, $m\pi + \pi/4$, and $m\pi + \pi/2$, respectively. Here the two cavities are identical with $\gamma_1 = 20\gamma_0$.

reflection is the sum of the two new resonances with the detuning $2\gamma_1$ and the identical decay rates.

(iii) When $\theta \neq m\pi/2$, for example, $\theta = \pi/4$, these two resonances possess distinct waveguide coupling strengths $\gamma_1(1 \pm \cos\theta)$. For example, $(1+\cos\theta) \gg (1-\cos\theta)$ for a certain θ. Thus, the mode with strong coupling represents a continuum while the mode with weak coupling plays the role of a discrete level. As a result, the Fano resonance line shape is produced by involving interference between the continuum and the discrete level, similar to the Fano-Anderson model. On the other hand, the two new resonances are also analogous to the bright and dark states in the atomic system. The mode with reflection coefficient r_1 approximately plays the role of a bright state (almost all light can be efficiently coupled to the bright-state mode and transported to the reflection), while the mode with reflection coefficient r_2 represents a dark state (the coupling to the dark-state mode is much weaker).

To further expose the essence of the asymmetric line shape, we turn to studying the phase angles of reflection amplitudes $r_{1,2}$. Thus, Eq. (11a) is rewritten as

$$r = e^{i\theta}(-|r_1|e^{i\varphi_1} + |r_2|e^{i\varphi_2}). \qquad (12)$$

Thus the total reflection rate reads

$$R = |r_1|^2 + |r_2|^2 - 2|r_1||r_2|\cos(\varphi_1 - \varphi_2). \qquad (13)$$

In Eq. (13), the first two terms represent the reflections of the two new resonances, and the last term denotes the interference between them. Figure 3(a) displays the phases $\varphi_{1,2}$ depending on the detuning $\Delta\omega$. It can be found that the phase difference $\varphi_2 - \varphi_1$ appears as a sharp change in the vicinity of $\Delta\omega = (\gamma_1 + \gamma_0/2)\tan\theta$. The total reflection also changes sharply in this region. This phenomenon is similar to the phase changes of discrete and continuum states in analyzing electron scattering [1]. Figure 3(b) plots the first two terms $|r_1|^2 + |r_2|^2$, the interference term $-2|r_1||r_2|\cos(\varphi_2 - \varphi_1)$, and the total reflection rate R. It is not difficult to find that the profile of $|r_1|^2 + |r_2|^2$ is the sum of reflections of the two new resonances, while the interference term behaves asymmetrically. As a result, the total reflection spectrum R is asymmetric.

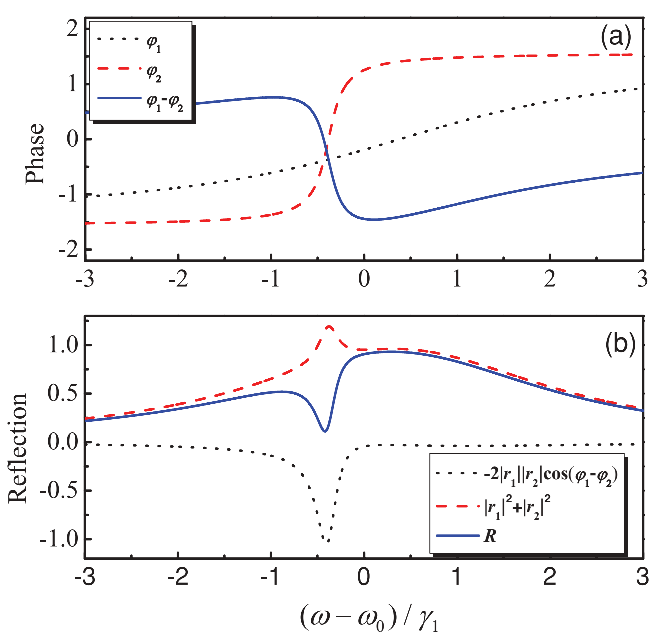

FIG. 3. (Color online) (a) Changes of phase φ_1 (dotted), φ_2 (dashed), and $\varphi_1 - \varphi_2$ (solid) depending on the detuning $\omega - \omega_0$. (b) The spectra of $|r_1|^2 + |r_2|^2$, $-2|r_1||r_2|\cos(\varphi_2 - \varphi_1)$, and R. For both cases, the two microcavities are identical with $\gamma_1 = 20\gamma_0$ and $\theta = m\pi + \pi/4$.

The sharp asymmetric line shape can improve the optical switching characteristics [9] and provide greatly enhanced slope sensitivity of biosensors [8,10,11], because the slope between zero and the unity reflection (or transmission) is greatly enhanced compared with that of a single resonator. In this kind of biosensor, the measurement is typically based on the shift of sharp Fano resonance. Thus, some environmental variations such as thermal fluctuations will insert the detection signal. As an alternative method, a measurement system could be constructed such that only one cavity is used as a sensing head, while the other plays the role of feedback. In this case, both cavities respond synchronously to the environmental variations because they are located in a microscale volume. As a result, the reflection spectrum of the coupled system has a shift (i.e., shifted spectrum), but no distortion of the line shape occurs [Fig. 4(a), from solid to dashed curves]. When target biomolecules interact with the sensing cavity, the reflection spectrum undergoes a distortion [Fig. 4(a), from solid to dotted curves]. Therefore, we can remove the effect of the environmental variations if we define this kind of spectrum aberrance as the sensing signal.

Finally, we show how to define the detection signal in such a distorted spectrum induced by binding biomolecules. To this end, we note that the Fano resonance dip has a remarkable change with the detuning ω_{12} between the two microcavities. In a realistic biosensing, ω_{12} only responds to the binding of target

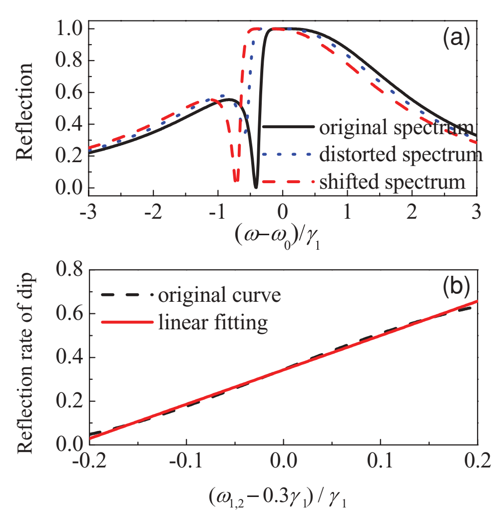

FIG. 4. (Color online) (a) Typical reflection spectra of the present Fano resonance. Solid, dashed, and dotted curves correspond to original, shifted ($\omega_{1,2}$ shift simultaneously from ω_0), and distorted cases (only ω_1 shifts from ω_0 and $\omega_2 = \omega_0$ remain unchanged), respectively. (b) The reflection rate of the Fano resonance dip depending on the detuning $\omega_{1,2}$ between the two microcavities. Here, the two cavities have an initial detuning of $0.3\gamma_1$. For both cases, $\gamma_1 = 20\gamma_0$ and $\theta = m\pi + \pi/16$.

biomolecules. Thus, the change of Fano resonance dip can be regarded as the detection signal. As shown in Fig. 4(b), the reflection rate of the Fano resonance dip responds linearly to the detuning ω_{12}. It should be noted here that we have assumed an initial bias detuning $0.3\gamma_1$ between the two microcavities for a better linearity.

In summary, we have investigated two single-mode microcavities side coupled to a common waveguide, and we obtained the indirect interaction strength between the two microcavities even when they are not directly coupled. This indirect interaction is mediated by the common waveguide, and the interaction parameter is dependent on the coupling strengths $\kappa_{1,j}$ and the propagating phase θ. This indirect interaction plays a key role in obtaining the asymmetric Fano line shape of the transport spectrum of the coupled system. Finally, we show that this sharp Fano line shape can be useful for highly sensitive sensing, and particularly, the sensing is immune to most environmental variations.

The authors acknowledge support from the National Science Foundation of China (No. 10821062 and No. 11004003) and the National Basic Research Program of China (Nos. 2007CB307001 and 2009CB930504). Yun-Feng Xiao was also supported by the Research Fund for the Doctoral Program of Higher Education (Grant No. 20090001120004).

[1] U. Fano, Phys. Rev. **124**, 1866 (1961).
[2] A. E. Miroshnichenko, S. Flach, and Y. S. Kivshar, Rev. Mod. Phys. **82**, 2257 (2010).
[3] K. J. Vahala, Nature (London) **424**, 839 (2003).
[4] H. A. Haus and Y. Lai, J. Lightwave Technol. **9**, 754 (1991).
[5] Y. Xu, Y. Li, R. K. Lee, and A. Yariv, Phys. Rev. E **62**, 7389 (2000).
[6] D. D. Smith, H. Chang, K. A. Fuller, A. T. Rosenberger, and R. W. Boyd, Phys. Rev. A **69**, 063804 (2004); A. Naweed, G. Farca, S. I. Shopova, and A. T. Rosenberger, *ibid.* **71**, 043804 (2005); J. K. Poon, L. Zhu, G. A. DeRose, and A. Yariv, Opt. Lett. **31**, 456 (2006); K. Totsuka, N. Kobayashi, and M. Tomita, Phys. Rev. Lett. **98**, 213904 (2007); M. Notomi, E. Kuramochi, and T. Tanabe, Nat. Photon. **2**, 741 (2008); S. I. Shopova, Y. Sun, A. T. Rosenberger, and X. Fan, Microfluid Nanofluid **6**, 425 (2009); Y. Dumeige, S. Trebaol, and P. Feron, Phys. Rev. A **79**, 013832 (2009).
[7] M. F. Yanik, W. Suh, Z. Wang, and S. Fan, Phys. Rev. Lett. **93**, 233903 (2004); L. Maleki, A. B. Matsko, A. A. Savchenkov, and V. S. Ilchenko, Opt. Lett. **29**, 626 (2004); P. Chak, S. Pereira, and J. E. Sipe, Phys. Rev. B **73**, 035105 (2006); Q. Xu, S. Sandhu, M. L. Povinelli, J. Shakya, S. Fan, and M. Lipson, Phys. Rev. Lett. **96**, 123901 (2006); Q. Xu, P. Dong, and M. Lipson, Nat. Phys. **3**, 406 (2007); Y.-F. Xiao, X.-B. Zou, W. Jiang, Y.-L. Chen, and G.-C. Guo, Phys. Rev. A **75**, 063833 (2007); S. F. Mingaleev, A. E. Miroshnichenko, and Y. S. Kivshar, Opt. Express **16**, 11647 (2008); X. Yang, M. Yu, D.-L. Kwong, and C. W. Wong, Phys. Rev. Lett. **102**, 173902 (2009).
[8] Y.-F. Xiao, V. Gaddam, and L. Yang, Opt. Express **16**, 12538 (2008).
[9] S. Fan, Appl. Phys. Lett. **80**, 908 (2002).
[10] C.-Y. Chao and L. J. Guo, Appl. Phys. Lett. **83**, 1527 (2003).
[11] W. M. N. Passaro and F. D. Leonardis, IEEE J. Sel. Top. Quantum Electron. **12**, 124 (2006).
[12] A. Chiba, H. Fujiwara, J. I. Hotta, S. Takeuchi, and K. Sasaki, Appl. Phys. Lett. **86**, 261106 (2005).
[13] Y.-F. Xiao, L. He, J. Zhu, and L. Yang, Appl. Phys. Lett. **94**, 231115 (2009).
[14] J. D. Franson and S. M. Hendrickson, Phys. Rev. A **74**, 053817 (2006).
[15] C. W. Gardiner and P. Zoller, *Quantum Noise*, 3rd ed. (Springer, Berlin, 2004).
[16] F. Le Kien, S. Dutta Gupta, K. P. Nayak, and K. Hakuta, Phys. Rev. A **72**, 063815 (2005).
[17] M. Hopmeier, W. Guss, M. Deussen, E. O. Gobel, and R. F. Mahrt, Phys. Rev. Lett. **82**, 4118 (1999).